

High Levels of Heat Transfer Coefficient During Convective Flow Boiling for R134a - EVR2021-0008

Rhandrey Maestri ^{1,*}, Guilherme Scagnolatto ¹, Cristiano B. Tibiriçá ¹

¹ University of São Paulo, EESC, Heat Transfer Research Group
São Carlos, SP, Brazil, 13566-590

* Rhandrey Maestri, rhandrey.maestri@usp.br

Abstract

This article presents new experimental convective heat transfer coefficient during flow boiling conditions for a microscale tube. The data were obtained in a horizontal 1.0 mm inside diameter stainless-steel tube with heating length of 100 mm, R-134a as working fluid, mass velocities ranging from 1990 to 5000 kg/m²s, heat flux from 109 to 382 kW/m² and heat transfer coefficient from 11.8 to 27.1 kW/m²-K. The experimental data were compared against the predictive method developed by Tibiriçá et al. (2017) and the results of the comparison are reported.

Keywords: R134a, flow boiling, microchannels

Introduction

The growing demand for dissipating high heat flux from present devices creates the need for new cooling technologies, as well as improvements in existing technologies. In order to increase the heat flux of a microchannel with single-phase cooling, maintaining the practical limits of the surface temperature, it is necessary to increase the heat transfer coefficient by increasing the flow rate or further decreasing the hydraulic diameter. Both are accompanied by very large increases in pressure drop. However, two-phase heat dissipation can achieve very high heat flux at a constant flow rate, maintaining a relatively constant surface temperature.

Initially, mechanical refrigeration was limited to a few applications with ammonia, sulfur dioxide and methyl chloride, which were the only refrigerants available, all highly toxic (Lecompte, 2015). With the exception of ammonia, all of these refrigerants have been replaced by halogenated hydrocarbons like R134a, R123 and R11, synthesized from the hydrocarbons of the methane and ethane series, which, due to their safety advantages, modernly constitute the refrigerants for most refrigeration installations.

Wojtan et al. (2006), Basu et al (2011) and Ali and Palm (2011) used R134a as working fluid and the first obtained the highest value of 600 kW/m² with 1540 kg/m²s in a 0.8 mm tube. Lazarek and Black (1982) achieved 336 kW/m² with R113 in a 3.15 mm tube and Katto and Yokoya (1984) could reach 411 kW/m² with R12 in a 5 mm tube.

Tibiriçá et al. (2012) presented experimental flow boiling heat transfer results for horizontal 1.0 and 2.2 mm stainless steel tubes for tests with R1234ze(E) and R134a with mass velocities ranging from 50 to 1500 kg/m²s and heat fluxes from 10 to 300 kW/m² using heated lengths of 180 mm and 361 mm.

Prediction of heat transfer coefficient (HTC) has been based mainly on correlations developed during the last

decades. Recently, Tibiriçá et al. (2017) tested 10 relevant prediction methods from the literature and developed a new correlation for two-phase flow conditions in microchannels. The database used for the correlation development is composed of 11 fluids with diameters ranging from 0.38 to 3 mm with a total of 3902 points. The correlation is easily implemented and had the best general performance predicting the database with an average error of 19%.

Taking this context into account, this paper presents new experimental data for HTC at high heat flux in 1.0 mm horizontal stainless steel tube. Tests were conducted with R134a for heated length of 100 mm. The experimental results were compared against the Tibiriçá et al. (2017) predictive method.

Experimental Apparatus

The experimental setup is comprised of refrigerant and water circuits. In the refrigerant circuit (Fig. 1), starting from the condenser, the test fluid flows through the filter passing by a Coriolis mass flow meter to the pump. Downstream of the pump, a bypass piping line containing a needle-valve is installed so that together with a frequency controller on the pump, the desired liquid flow rate can be set. Just upstream of the preheater inlet, the enthalpy of the liquid is estimated from its temperature by a thermocouple located at an adiabatic position on the outside tube wall, and its pressure by an absolute pressure transducer.

In the reservoir, fluid is heated up to the desired saturation pressure. The test section is made of a unique horizontal stainless steel tube heated by applying direct DC current to its surface and it is thermally insulated. Once the liquid leaves the test section its temperature is determined from a thermocouple located on the external tube surface. Then, the fluid is directed to a tube-in-tube type heat exchanger where it is condensed and subcooled.

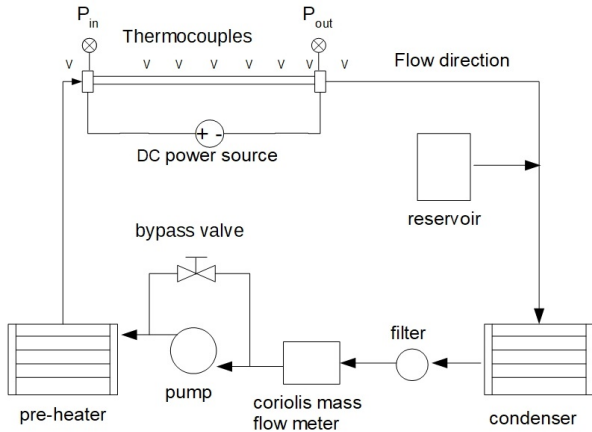


Figure 1: Test facility diagram used for experiments

The wall temperatures are measured through six thermocouples fixed along the outside wall of the test section as indicated in Fig. 2.

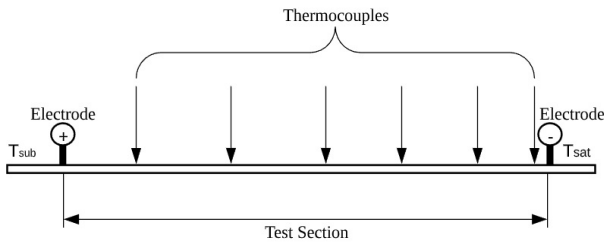


Figure 2: Test section details

The experiments were conducted first by setting the temperature in the refrigerant tank. Once establishing the saturation pressure in the refrigerant circuit, the mass velocity was set through the frequency controller acting on the pump. Heat flux was then applied to the test section to initiate evaporation. The power applied in the test section was incremented in small steps, always controlling other parameters to keep them constant. For the tests performed in this article, measurements were made by increasing the heat flux until the thermocouples located at the end of the test section show sudden overheating. Such a procedure was used to avoid failure of the test section due to wall temperature oscillations.

Data reduction

In the present study, the experimental parameters influencing the HTC are heat flux, exit saturation temperature, mass velocity and local vapor quality. The data reduction is similar to one performed in the work of Tibiriçá et al. (2012). The heat flux (q) is given by the ratio between the electrical power supplied to the test section and its internal area based on the heated length and inside diameter. Mass velocity is given by the ratio between the mass flow rate given by the Coriolis and the internal cross-sectional area of the tube. The electrical power is given by the product between the electrical current and the voltage supplied by the DC power source. Local heat transfer coefficients were calculated according to the Newton's cooling law as follows:

$$h_{local} = \frac{q}{T_w - T_{sat}(z)} \quad (1)$$

where T_w is the surface temperature of the inner tube wall estimated according to the Fourier's law based on the outer wall temperature measurements and assuming one-dimensional conduction through difference between readings of inlet and outlet thermocouples. For that it was assumed internal uniform heat generation in the wall and an adiabatic external surface. T_{sat} is the refrigerant local saturation temperature. The local saturation temperature is estimated through the temperature at the beginning of the test section and the rate between the location of the thermocouple in the test section together with the total temperature variation, given by the difference between the temperature of the inlet and outlet.

The vapor quality at a specific position z in the test section was determined by an energy balance over the pre-heater and the test section according to the following equation:

$$x(z) = \frac{(q \pi D z / \dot{m}) + i_{ins} - i_L(z)}{i_{lv}} \quad (2)$$

The enthalpy of the liquid at the inlet of the pre-heater, i_{ins} , was estimated based on the measured temperature and pressure at the inlet. The liquid enthalpy and latent heat of vaporization at the position z , $i_{lv(z)}$ and $i_L(z)$, respectively, were estimated based on the fluid temperature measured at position (z) and assuming a saturated state. In Eq. (2), q is the heat flux.

Experimental validation and uncertainties

Uncertainties for parameters involved in the experiment were estimated using the method of sequential perturbation, according to Moffat (1988). All thermocouples were calibrated and the temperature uncertainty was evaluated according to the procedure suggested by Abernethy and Thompson (1973). The experimental uncertainties are listed in Table 1, depicting the uncertainties of the measured and calculated parameters and including the maximum uncertainties of the vapor quality and heat transfer coefficient. To calculate the uncertainties of the estimated vapor qualities, were assumed heat losses of 10%. As shown in Fig. 3 the experimental data of single-phase falls between the 10% region when running with mass velocities greater than 4000 kg/m²s for exit temperature of 30 °C.

Table 1: Uncertainty of measured and calculated parameters

Parameter	Uncertainty	Parameter	Uncertainty
D	20 μm	x	< 10%
L	0.2 mm	p	1 kPa
G	0.8 %	T	0.5 °C
q	< 4%	h	5 – 20%

It must be mentioned that during two-phase flow, heat losses are lower than during single-phase flow due to a much higher internal heat transfer coefficient.

In order to calculate the heat transfer coefficient uncertainties, heat losses to the environment were neglected. Single-phase flow experiments were performed to assure the accuracy of the estimated vapor quality and evaluate the effective rate of heat transferred to the single phase refrigerant, defined as follows:

$$\Delta E/E = \frac{(\pi D^2/4)G(i_{out} - i_{ins}) - P}{P} \quad (3)$$

where P is the electrical power supplied by the DC power source to the heated section. Fig. 3 shows the energy balance results under turbulent subcooled liquid flow conditions. According to these tests, the heat losses during the single-phase experiments were below 10%.

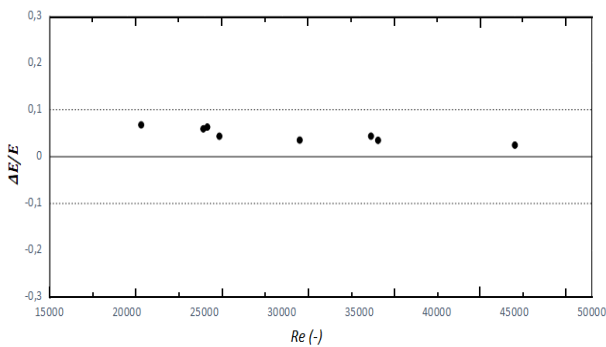


Figure 3: Single-phase energy balance for R134a

Single-phase heat transfer experiments were also performed to validate the test facility. Fig. 4 shows agreements of the Gnielinski (1975) correlation for almost all experimental data and better agreement of Dittus (1985) correlation for lower Reynolds number.

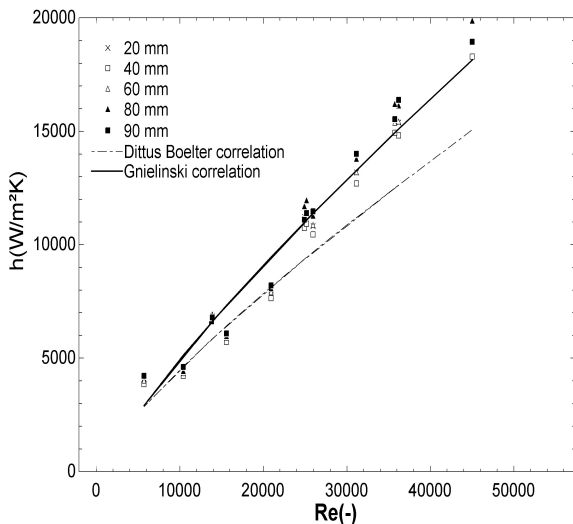


Figure 4: Single phase heat transfer comparison

Experimental results

In this section, 45 experimental points obtained with two-phase flow are described, as constant mass velocities

was not maintained during increments of heat flux, maps of experimental points are presented. Table 2 presents experimental operating parameters.

Table 2: Operating parameters of study

Mass velocity	Heat flux	Outlet quality
kg/m²s	kW/m²	(-)
1990 – 5000	109 – 382	0 – 0.23

Figure 5 shows heat transfer coefficient results with increasing heat flux in three different axial positions of the test section. It is clear that an increase in heat flux causes an increase in HTC. The figure shows that the experimental facility was able to provide HTC values close to 27500 W/m²K.

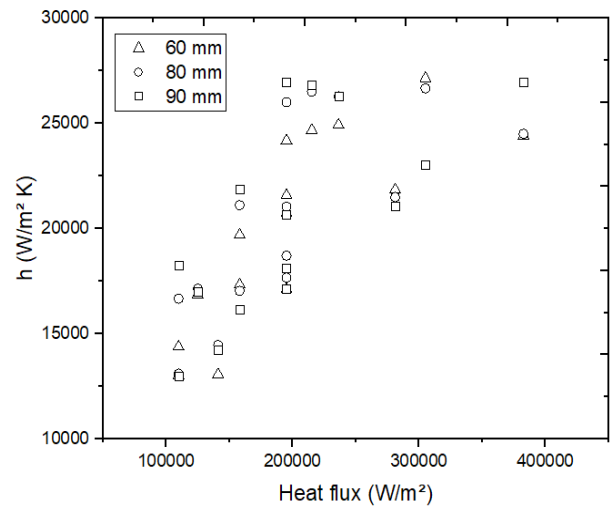


Figure 5 : Effect of heat flux on HTC

Figure 6 shows heat transfer coefficient results with local vapor quality in three different axial positions of the test section.

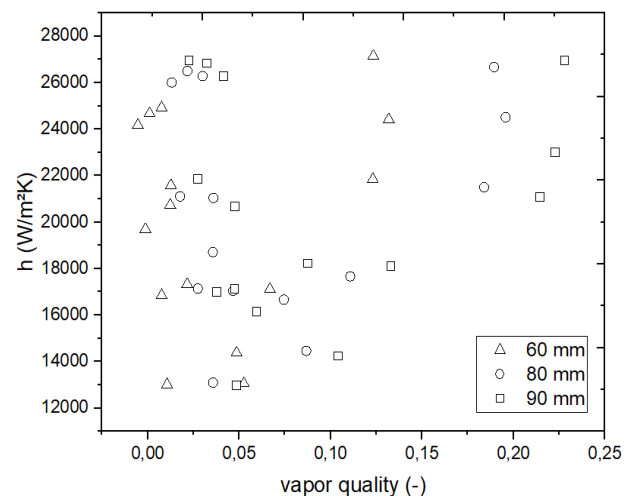


Figure 6: Map of HTC with local vapor quality

In order to evaluate the capability of heat transfer correlations to predict the present database, a comparison between the experimental data and Tibiriça et al (2017) correlation was performed. The predictive method are evaluated according to the fraction of data predicted within 30% error band. Fig. 8 shows a comparison between the experimental results and the predictions given by the correlation. All the predicted data fall within an error band of $\pm 30\%$.

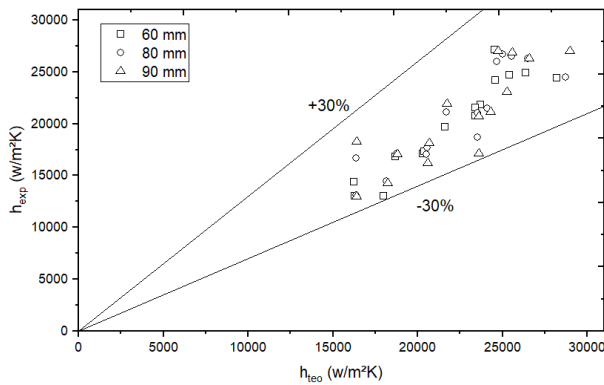


Figure 8: Comparison of Tibiriça et al (2017) correlation and the heat transfer experimental data

Conclusions

This paper has presented a new experimental apparatus created in the Heat Transfer Research Group of EESC-USP and discussed new flow boiling heat transfer coefficient data for R134a in 1.0 mm circular channel. The experimental results reached high values of heat flux as close to 400 kW/m² and the goal of obtaining HTC values of up to 27 kW/m²K was achieved due to the combination of high mass flow rates and high electrical power, beyond that, higher values of heat flux will be obtained in future works. The experimental results were compared against the predictive method of Tibiriça et al. (2017) providing a good accuracy predicting the database with a mean absolute error of about 14%.

Acknowledgements

The authors acknowledge CAPES (Coordination for the Improvement of Higher Education Personnel, Finance Code 001), CNPq (National Council for Scientific and Technological Development, process 304972/2017-7) and FAPESP (São Paulo Research Foundation, 2019/11066-9), for funding researches that have contributed to this study.

References

- Abernethy, R. B., and Thompson, J. W., 1973, Handbook Uncertainty in Gas Turbine Measurements, Arnold Engineering Development Center, Arnold Air Force Station, TN
- Gnielinski, Volker. (1975) New equations for heat and mass transfer in the turbulent flow in pipes and channels. STIA, v. 41, n. 1, p. 8-16.
- G.M. Lazarek, S.H. Black, (1982) Evaporative heat transfer, pressure drop and critical heat flux in a small vertical tube with R-113, Int. J. Heat Mass Transf. 25 945–960.

- Y. Katto, S. Yokoya, (1984), Critical heat flux of liquid helium (I) in forced convective boiling, Int. J. Multiph. Flow. 10 401–413.
- Dittus, F. W.; Boelter, L. M. K. (1985) Heat transfer in automobile radiators of the tubular type. International Communications in Heat and Mass Transfer, v. 12, n. 1, p. 3-22.
- Moffat, R. J., 1988, “Describing the Uncertainties in Experimental Results,” Exp. Thermal Fluid Sci., 1, pp. 3–17.
- L. Wojtan, R. Revellin, J.R. Thome, (2006), Investigation of saturated critical heat flux in a single, uniformly heated microchannel, Exp. Therm. Fluid Sci. 30 765–774.
- S. Basu, S. Ndao, G.J. Michna, Y. Peles, M.K. Jensen, (2011), Flow boiling of R134a in circular microtubes— Part I: Study of heat transfer characteristics, ASME J. Heat Transf. 133 1–9.
- R. Ali, B. Palm, (2011), Dryout characteristics during flow boiling of R134a in vertical circular minichannels, Int. J. Heat Mass Transf. 54 2434–2445.
- Bigonha Tibiriça, Cristiano, Gherhardt Ribatski, and John Richard Thome. (2012) "Flow boiling characteristics for R1234ze (E) in 1.0 and 2.2 mm circular channels." Journal of heat transfer 134.2.
- C.L. Ong, J.R. Thome, (2011) Macro-to-microchannel transition in two-phase flow: Part 2 – Flow boiling heat transfer and critical heat flux, Exp. Therm. Fluid Sci. 35 873–886.
- Tibiriça, C. B.; Rocha, D. M. ; Sueth Jr., I. L. S. ; Bochio, G.; Shimizu, G. K. K. ; Barbosa, M. C. ; Ferreira, S. S. (2017). A complete set of simple and optimized correlations for microchannel flow boiling and two-phase flow applications. Applied Thermal Engineering, v. 126, p. 774-795

Disclaimer

The authors are solely responsible for the material included in this document.